Model for Demagnetization-Induced Noise in Thin-Film Magnetic Recording Media

ROMNEY R. KATTI, MEMBER, IEEE, VENUGOPAL V. VEERAVALLI,
MARK H. KRYDER, SENIOR MEMBER, IEEE, AND
B. V. K. VIJAYA KUMAR, MEMBER, IEEE

Abstract—**A linear, statistical model is described which predicts the power spectrum of measured noise in bulk-demagnetized (i.e., ac-erased) thin-film magnetic recording media. It is shown that the noise is the result of magnetic flux which is ascribed to erasure-induced transitions along the track length in the medium. The noise power spectrum for a rigid disk medium is shown to correspond to the power spectrum of Poisson-distributed induced transitions along the track length, while noise along the track width is sufficiently described in terms of a uniform, average magnetization with small variance. Experimental data from two thin-film disks are used with the model to estimate the Poisson parameter for each disk. It is demonstrated that dc-erased noise from particulate media can be considered as a limiting case of the Poisson model.**

I. Introduction

PREVIOUS WORK has shown that ac-erased noise in particulate media can be represented as a white noise process at the input of the magnetic recording channel [1], [2]. Signal-dependent noise has been considered with a variety of analyses for particulate [3]–[6] and thin-film disks [7]–[11]. Noise due to reverse dc-erase processses has also been observed [12] and analyzed [13] using a recording theory approach. It has also been observed that ac-erased noise power in thin-film disks is greater than dc-erased noise power.

The purpose of this work is to show that ac-erasure-induced noise along the direction of the track length in both thin-film and particulate magnetic recording disks can be treated as a response to a statistical process, where the noise statistics along the track width may be assumed to be uniform. The noise measured along the track length cannot be explained simply as a white-noise process in thin-film disks, but can be explained by using some more general process. It is shown that a Poisson process accurately describes the observed power spectra. The Poisson parameter is estimated experimentally herein for two thin-film disks. The Poisson model should assist in a better understanding of the noise from thin-film disks, with the Poisson parameter serving as a useful measure in evaluating the uniformity of the media.

Manuscript received October 26, 1987; revised March 1, 1988.

R. R. Katti was with the Magnetics Technology Center, Carnegie Mellon University, Pittsburgh, PA 15213-3890. He is now at the Jet Propulsion Laboratory, Pasadena, CA 91109.

V. V. Veeravalli was with the Magnetics Technology Center, Carnegie Mellon University, Pittsburgh, PA 15213-3890. He is now with the Coordinated Science Laboratory, University of Illinois, Urbana, IL 61801.

M. H. Kryder and B. V. K. Vijaya Kumar are with the Magnetics Technology Center, Carnegie Mellon University, Pittsburgh, PA 15213-3890.

IEEE Log Number 8821228.

II. Physical Model

It is assumed in the model that a recording head detects flux which emanates from transitions which occur along the track of a disk, where a transition is defined as a source of diverging magnetization. A readback channel is assumed to exist which differentiates the flux from the magnetization pattern and which introduces readback losses before producing an output signal. This process is depicted schematically in Fig. 1, where Fig. 1(a) depicts an effective magnetization pattern, Fig. 1(b) depicts the differentiated flux pattern, and Fig. 1(c) depicts the output signal which is a consequence of the convolution of the readback signal from the isolated pulse with the differentiated flux sequence [10]. It is assumed that the bandwidth of the signal amplifiers is significantly greater than that of the recording head, so that the frequency-dependent effects of the amplifiers are negligible and that the dominant sources of frequency-dependent effects are the head, medium, and head–medium interface.

The model assumes for thin-film media that variations in coercivity exist in the film such that *regions* of reversed magnetization (e.g., ensembles of domains) can be formed in typically high-squareness material on the basis of variations in applied magnetic fields. Consider a longitudinally oriented, alternating erase field with a decaying envelope, as shown in Fig. 2. Shown also in the figure are two adjacent regions with opposing magnetization, numbered (1) and (2), with given magnetizations and slightly different coercivities, numbered H_{C1} and H_{C2}. Since a decaying, alternating erase field reverses polarity during each half-cycle, then a sufficiently large peak field amplitude (compared to the coercivity) in one direction should align the magnetization of the two adjacent regions, and a diminished but still large peak field amplitude in the opposite direction a half-cycle later should reverse the magnetization of both regions. This behavior is illustrated in the first two half-cycles in the figure, and is useful in depicting the lower noise, dc-erased state. It is noted that the low noise level in the dc-erase state is taken to mean that variations in $4\pi M_R$ are negligible.

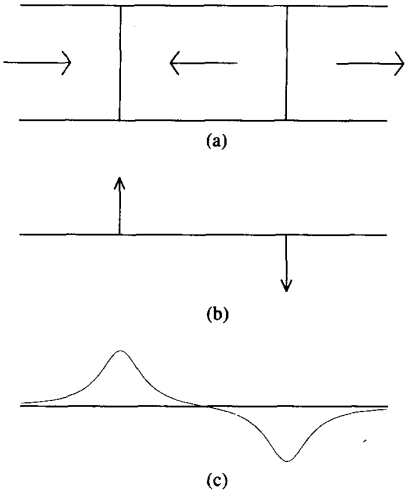

Fig. 1. The readback signal process, from (a) the effective magnetization pattern, to (b) the differentiated flux sequence, to (c) the observed read signal.

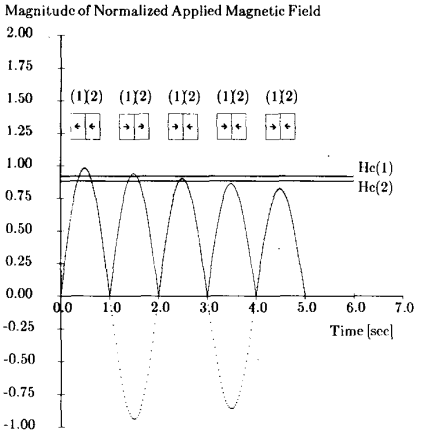

Fig. 2. Schematic of ac-erasure-induced transitions in thin-film media. The solid curves indicate the magnitude of the erase field, while dotted curves indicate the actual applied erase field.

For some particular envelope decay rate, a peak field amplitude with sufficiently large amplitude will arise where the peak field amplitude in the next half-cycle will have some amplitude between the two coercivities of the two regions. This is illustrated in Fig. 2 with the second and third half-cycles. At this point, a transition is induced between the regions, and it is assumed that these magnetized regions do not demagnetize themselves. If the field continues to decay at a sufficiently rapid rate so that the magnetized region that has most recently reversed will not reverse again (or, alternatively, if the field diminishes so that an odd number of reversals occur), then the transition will be maintained. This sequence is shown in the third, fourth, and fifth half-cycles.

Magnetized regions, with magnetization directed parallel to the track (i.e., parallel to the applied erase field direction), are assumed to be distributed throughout the medium. Variations in the matrix of magnetized regions along the width of the track to reduce the net flux seen by the recording head (which has a nominal width) from that corresponding to saturated magnetization to that of some smaller value of magnetization, since some magnetized regions point in one direction and others point oppositely. Since the recording head is detecting an average value of flux, the statistics along the track width are assumed to be uniform.

Variations in the matrix of magnetized regions along the track direction produce minute transitions that occur with a pattern which is characteristic of some statistical distribution. Such induced transitions produce demagnetizing fields which induce a signal in the recording head. The absolute value of the magnetization between transitions can initially be considered as a random variable that assumes values between zero and the saturation value of the magnetization. A conceptualization of the ac-erasure-induced transitions and the corresponding magnetization pattern, $m(t)$, is shown in Fig. 3(a) and (b), respectively, where the function $m(t)$ represents a time-dependent random process whose statistics are derived in the next section.

III. Power Spectra Calculations

The sequence of transitions $m(t)$, which is produced by ac-erasure, is sensed through the magnetic recording channel to produce the ac-erasure-induced noise. Derived here are the power spectral densities of the random process $m(t)$ and of the noise it produces at the output of the magnetic recording channel.

The power spectral density $S_m(\omega)$ of a stationary, zero-mean random process $m(t)$ is defined as the Fourier transform of $R_m(\tau)$, where $R_m(\tau)$ is the autocorrelation function of $m(t)$, which describes the second-order statistics of $m(t)$. The autocorrelation function is defined by

$$R_m(\tau) = E\{m(t)\, m(t+\tau)\} \tag{1}$$

where $E\{\cdot\}$ denotes the operation of statistical expectation.

The random process $m(t)$ represents the input magnetization pattern. The function $m(t)$ may assume values in the interval $[-M_s, +M_s]$, where M_s is the saturation value of the magnetization. The value of $m(t)$ is assumed to be constant between transitions, as shown conceptually in Fig. 3(b). The absolute value of the magnetization between transitions is a random variable M, which can take on values in the interval $[0, M_s]$. Let $E\{M\}$ and $V\{M\}$ denote the mean and variance, respectively, of this random variable.

The transitions which define $m(t)$ are assumed to occur with an average frequency of λ transitions per second. It is now assumed that the positions at which these transitions occur form a Poisson point process [14] with parameter λ. The justification for this assumption is that the probability of having more than one transition in an interval of length dt tends to zero faster than dt tends to zero, since it is not possible for more than one transition

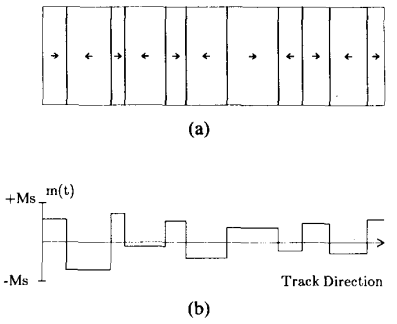

Fig. 3. (a) Conceptual erasure-induced transition pattern, where each magnetized region is composed of arbitrarily directed saturated domains. (b) Corresponding magnetization as a function of time, for the case where a nonzero variance is associated with the amplitude of $m(t)$.

to occur at a given time [14]. It is noted that the Poisson assumption is borrowed from a similar analysis that has been done in the past for random telegraphic signals [14]. The probability that the number of transitions equals k in an interval of duration t is given by

$$p(k) = \frac{e^{-\lambda t}(\lambda t)^k}{k!}, \qquad k = 0, 1, 2, \cdots. \tag{2}$$

To continue this analysis, it is assumed that $m(0)$ is positive. Then, $m(t)$ is positive if the number of transitions in the time interval $(0, t)$ is even. Similarly, $m(t)$ is negative if the number of transitions in $(0, t)$ is odd. Hence, the following probabilities are obtained:

$$\begin{aligned} P\{m(t) > 0\} &= p(0) + p(2) + \cdots \\ &= e^{-\lambda t}\left[1 + \frac{(\lambda t)^2}{2!} + \cdots\right] \\ &= e^{-\lambda t}\cosh(\lambda t) \end{aligned} \tag{3}$$

and

$$\begin{aligned} P\{m(t) < 0\} &= p(1) + p(3) + \cdots \\ &= e^{-\lambda t}\left[\lambda t + \frac{(\lambda t)^3}{3!} + \cdots\right] \\ &= e^{-\lambda t}\sinh(\lambda t). \end{aligned} \tag{4}$$

Using (3) and (4), the statistics of the random process $m(t)$ are now derived. The expected value of the random process $m(t)$ is decomposed into the following expression:

$$\begin{aligned} E\{m(t)\} &= E\{m(t)\,|\,m(t) > 0\} \cdot P\{m(t) > 0\} \\ &\quad + E\{m(t)\,|\,m(t) < 0\} \cdot P\{m(t) < 0\} \\ &= E\{M\}(\cosh \lambda t - \sinh \lambda t)\, e^{-\lambda t} \\ &= E\{M\}\, e^{-2\lambda t}. \end{aligned} \tag{5}$$

Since $m(0)$ was assumed to be positive, $E\{m(t)\}$ is positive. If $m(0)$ were assumed to be negative, $E\{m(t)\}$ would be precisely the negative of the value in (5). Since $m(0)$ can be either negative or positive with equal probability, it follows that $m(t)$ is a zero-mean random process.

The function $E\{m(t)\, m(t + \tau)\}$ is now evaluated. If there are no transitions in the interval $[t, t + \tau]$, then $m(t)$ and $m(t + \tau)$ are the same random variable. It is assumed that when a finite number of transitions occurs between t and $t + \tau$, the random variables $m(t)$ and $m(t + \tau)$ have magnitudes which are uncorrelated; only the signs of these random variables are correlated.

It is shown in the Appendix that the autocorrelation function of $m(t)$ can be expressed as the sum of two decaying exponentials

$$R_m(\tau) = V\{M\}\, e^{-\lambda|\tau|} + E\{M\}^2 e^{-2\lambda|\tau|}. \tag{6}$$

Taking the Fourier transform of $R_m(\tau)$ with respect to τ, the power spectral density $S_m(\omega)$ of the random process $m(t)$ is written as

$$S_m(\omega) = E\{M\}^2 \frac{4\lambda}{\omega^2 + 4\lambda^2} + V\{M\} \frac{2\lambda}{\omega^2 + \lambda^2}. \tag{7}$$

Equation (7) defines the power spectral density of the Poisson input sequence $m(t)$. The erasure-induced noise measured at the output is the response of the magnetic recording channel to the input sequence $m(t)$. A Lorentzian pulse shape model [15] is used here to represent the inductive magnetic recording channel. The response of the magnetic recording channel to an idealized transition is a Lorentzian pulse given by

$$r(t) = 2A \frac{\sigma}{t^2 + \sigma^2} \tag{8}$$

where 2σ is the PW_{50} of the pulse [16], and A is the amplitude factor.

The Fourier transform of $r(t)$ is the decaying exponential given by

$$R(\omega) = 2\pi A e^{-\sigma|\omega|}. \tag{9}$$

The term $R(\omega)$ broadens and reduces the amplitude of idealized transitions, and represents the *channel loss response*. The function used on the right-hand side of (9) can equivalently be deduced as the Fourier transform of the Karlquist head field, for recording heads with small gap lengths such as those used here.

The magnetic recording channel under consideration here includes the spacing and transition loss terms in the parameter σ, so that (8) can be considered as the response of an idealized normalized transition which bounds negatively saturated (with normalized amplitude -1) and positively saturated (with normalized amplitude $+1$) regions. Hence, the channel transfer function $H(\omega)$, which is the Fourier transform of the impulse response of the channel, is given in terms of $R(\omega)$ as

$$H(\omega) = \frac{j\omega}{2} R(\omega) = j\pi A \omega e^{-\sigma|\omega|}. \tag{10}$$

The power spectral density of the noise at the output of the magnetic recording channel with $m(t)$ as input is then

given by [14]

$$S_n(\omega) = S_m(\omega)\left|H(\omega)\right|^2 = A^2\pi^2\omega^2 e^{-2\sigma|\omega|} \cdot \left[E\{M\}^2 \frac{4\lambda}{\omega^2 + 4\lambda^2} + V\{M\}\frac{2\lambda}{\omega^2 + \lambda^2}\right]. \quad (11)$$

IV. Experimental Method

To conduct the experimentation, magnetic recording disks were mounted on a magnetic recording test stand and subjected to erasure and/or signal writing, and the signals and noise were read, amplified, and detected. A schematic of this system is shown in Fig. 4. The characteristics of the recording head are given in Table I, and the characteristics of the media are given in Table II. Recording head signals were amplified with an NE592 preamplifier and an HP8447A buffer amplifier, and the signals were detected with an HP8568B Spectrum Analyzer. The spectrum analyzer used heterodyne detection and swept a narrow-bandwidth, analog filter across a wider frequency band to measure the root-mean-square (rms) voltage as a function of frequency. The rms voltage measured with the spectrum analyzer is proportional to the square root of the power spectral density [10], so that the following function was measured:

$$\left|S_n(\omega)\right|^{1/2} = \alpha\omega e^{-\sigma|\omega|}\left[E\{M\}^2\frac{4\lambda}{\omega^2 + 4\lambda^2} + V\{M\}\frac{2\lambda}{\omega^2 + \lambda^2}\right]^{1/2}. \quad (12)$$

The measured spectra were then digitized to accommodate storage and data processing. The settings for the spectrum analyzer that were used are given in Table III.

The channel response as a function of frequency was measured for each disk and recording head combination, to estimate the parameters α and σ. To measure the amplitude factor α, saturated, NRZI-All-1 patterns were written, where the write current to the recording head was optimized for transitions written at 1.0 MHz, and the rms voltage amplitude of the fundamental was measured with a spectrum analyzer. The transition parameter σ was measured by measuring the half-width of isolated pulses in the time domain from a 100-MHz Tektronix 2235 oscilloscope, as shown in Fig. 5. This value of σ will be denoted as σ_{PW50}. To check for consistency in measuring σ, the spectrum for jitter noise in thin-film media, as defined by Belk *et al.* [8], Madrid *et al.* [10], and Moon *et al.* [11], was also measured. Since the jitter noise spectrum, which comprises the broad-band modulation noise spectrum, should match that of the channel, the value for the transition parameter, defined here as σ_{jitter}, can also be measured in this way. By writing an NRZI-All-1 pattern as discussed above, the resulting jitter noise signal spectrum can be measured on a spectrum analyzer. A typical

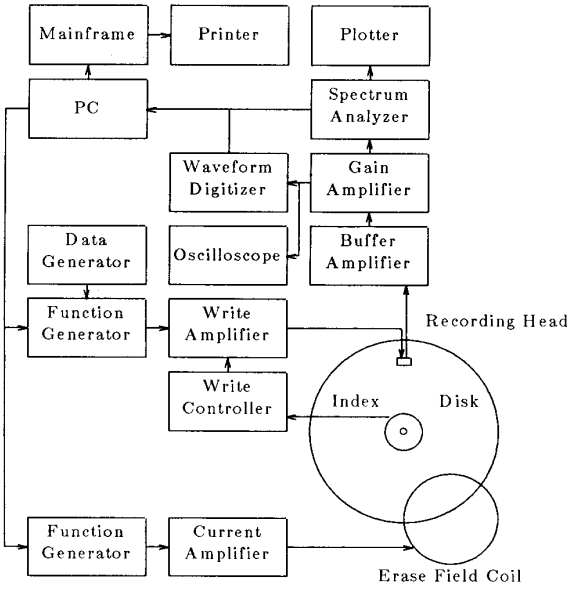

Fig. 4. Apparatus for measuring power spectra.

TABLE I
Recording Head Characteristics

Head Parameter	Parameter Value
Head type	inductive Mn-Zn ferrite
Gap length	0.4 ± 0.1 μm
Track width	250 ± 5 μm
Turns bifilar	13/13
Head current, disk *A*	20 $mA_{o\text{-}p}$ at 1.0 MHz
Head current, disk *B*	20 $mA_{o\text{-}p}$ at 1.0 MHz
Head current, disk *C*	35 $mA_{o\text{-}p}$ at 1.0 MHz
Flying height	0.45 μm ± 0.075 μm at 3600 r/min
Track radius	6.1 cm
Angular velocity	3600 r/min

TABLE II
Media Characteristics

Diameter: 5.25 in Disk	Coercivity, Magnetic Layer Thickness
A sputtered Co-Ni thin film	650 Oe, 625 Å
B sputtered Co-Ni-Pt thin film	830 Oe, 650 Å
C Particulate Co-γ-Fe_2O_3	750 Oe, 0.75 μm

TABLE III
Spectrum Analyzer Settings for Channel Response and Noise Measurements

Amplifier Gain into Spectrum Analyzer: 80			
Pattern	Frequency Range (MHz)	Slot Bandwidth (kHz)	Sweep Time (s)
Signal	0.0-0.1	0.1	20
Signal	0.0-1.0	1.0	20
Signal	0-10.0	10.0	20
Noise	0-10	10.0	200

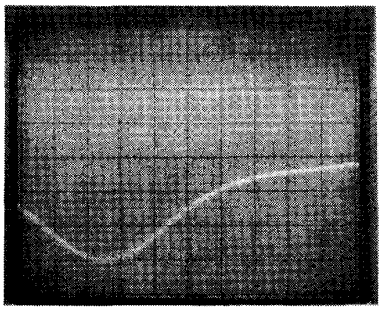

Fig. 5. Oscilloscope photograph of a read pulse from thin-film disk *A*. Horizontal scale is 20 ns/div. The hashed time axis is the 0-V baseline.

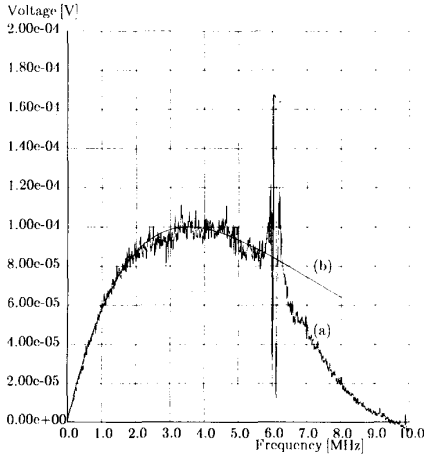

Fig. 6. Jitter-noise spectrum for measuring channel response: (*a*) measured jitter-noise response for disk *A*, and (*b*) peak-normalized channel response fit.

jitter noise spectrum, along with a portion of the fundamental signal, is shown in Fig. 6 for a thin-film disk.

The power spectrum of the channel loss response was separately measured by reading an NRZI-All-1's pattern. A square-wave pattern composed of isolated transitions was written at 250 kHz. The measured power spectrum is shown in Fig. 11(*b*).

The bulk-ac-erasure-induced noise response was measured by using a decaying ac magnetic field to bulk demagnetize the disks, and by using a spectrum analyzer to measure the amplified noise voltage read by the recording head. Thin-film and particulate disks were subjected to ac magnetic field erasure by an electromagnet shown schematically in Fig. 7. The erasure waveform was a computer-controlled, 0.5-Hz sinusoid which had an envelope that decayed linearly at the rate of 7 Oe/s. Unless noted otherwise for erasure induced with a recording head, it will be assumed that ac-erasure was achieved in the bulk due to this type of procedure. After ac-erasure, the signals were read, amplified, and detected with the spectrum analyzer. Background noise voltage due to the electronics, recording head, and stray sources was subtracted digitally from the ac-erasure-induced spectra, so that the presented data reflect channel-modified media noise.

The head-ac-erasure-induced noise response was measured as above, except that an ac magnetic field from a recording head was used to demagnetize the disks locally.

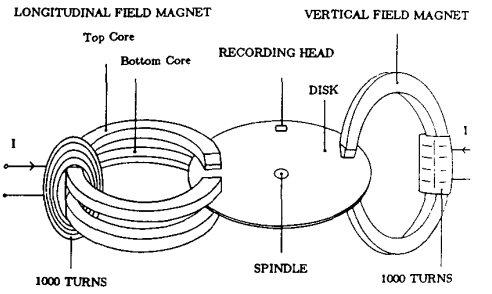

Fig. 7. Apparatus for inducing erasure.

The frequency of the erase current was 8.0 MHz, and the head was passed in contact along the track at a rate of approximately 1.0 cm/s. These values were chosen since they produced an envelope for the ac-erase waveform which decayed at a rate of approximately 5 Oe/cycle for magnetic field values near the coercivity, assuming the Karlqvist approximation [17] to represent the head field and the head field gradient.

V. Experimental Results

The measured, bulk-ac-erasure-induced noise for thin-film disk *A* is shown in Fig. 8(*a*). A curve fit to (12), using the parameters given in Table IV, is shown in Fig. 8(*b*). A normalized plot of the channel response as given by (10) is shown in Fig. 8(*c*), for the parameters given in Table IV. The measured noise responses, curve fits, and peak-normalized channel responses for thin-film disk *B* and particulate disk *C* are shown in Figs. 9 and 10, respectively.

The measured channel loss response corresponding to $R(\omega)$ is shown in Fig. 11(*b*). Since the vertical scale is in decibels and the horizontal scale varies linearly with frequency, the envelope of an exponential function, as indicated in Fig. 11(*a*), will appear as a straight line. It is observed that the envelope of the measured data deviates from the envelope corresponding to the ideal Lorentzian channel at a frequency in excess of 5 MHz. These losses represent additional losses due to the recording head.

The measured, head-ac-erasure-induced noise for thin-film disk *A* is shown in Fig. 12. A curve fit to (12), using the parameters given in Table IV, is also shown in Fig. 12.

VI. Discussion

A comparison between the measured noise data for thin-film disks in Figs. 8 and 9 and (12), which is favorable for the most part, reveals the following observations in the four frequency bands corresponding to low, moderate, moderately high, and high frequencies. At low frequencies, a linear dependence is exhibited between voltage and frequency, so that the response of an ideal recording head is realized. At moderate frequencies, a peak occurs in the noise spectrum, and the frequency of the peak is less than that predicted simply by the channel. The ac-erasure-induced noise therefore does not follow the statistics of a white-noise process, but does correspond to a Poisson process with parameters given in Table IV. At moderately high frequencies, the linear frequency dependence of head

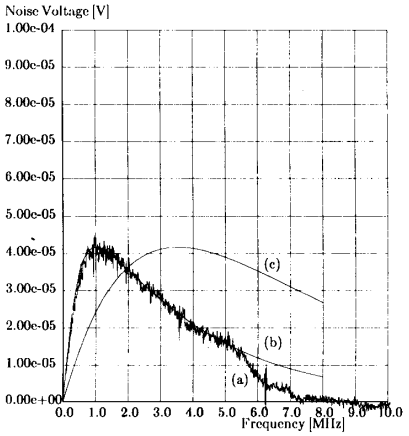

Fig. 8. Experimental data for disk *A*: (*a*) measured bulk-erasure-induced noise data; (*b*) model curve fit to data; and (*c*) peak-amplitude-normalized channel response.

TABLE IV
EXPERIMENTAL VALUES FOR MODEL PARAMETERS

Parameter	Disk *A**	Disk *B**	Disk *C**	Disk *A***
σ_{PW50}(ns)	48 ± 4	44 ± 4	84 ± 4	48 ± 4
σ_{fitted}(ns)	45	40	84	45
α(V/MHz)	0.104	0.112	0.169	0.104
$E\{M\}$	0.00140	0.00151	3.73×10^{-5}	0.00122
$V\{M\}$	"0"	"0"	"0"	"0"
λ(MHz)	2.0	4.0	≥50	5

*Demagnetization induced in the bulk.
**Demagnetization induced with the recording head.

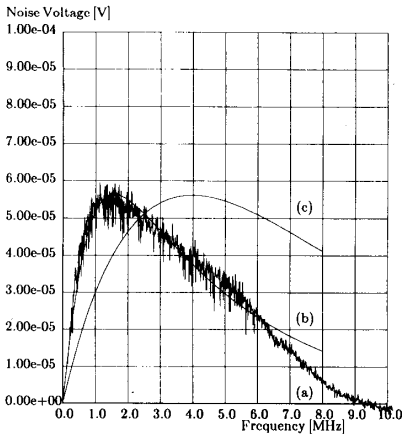

Fig. 9. Experimental data for disk *B*: (*a*) measured bulk-erasure-induced noise data; (*b*) model curve fit to data; and (*c*) peak-amplitude-normalized channel response.

differentiation is canceled by the inverse-frequency dependence of the Poisson process, so that the output follows the channel loss response.

At high frequencies, the noise spectrum predicted by the model deviates from the measured response. The discrepancy occurs because the measured channel response deviates from the idealized Lorentzian representation used in the present analysis. This feature is observed by comparing the difference in the channel response predicted by jitter noise against the idealized Lorentzian channel response, as shown in Fig. 6. Note that the frequency where the actual and idealized channel responses deviate in Fig. 6 is close to the frequency in Fig. 8 where a similar deviation occurs. Further, the measured spectrum of a sequence of isolated transitions is shown in Fig. 11(*b*), where the vertical scale in the figure is given in decibels so that a linear envelope as shown in Fig. 11(*a*) for odd harmonics corresponds to Lorentzian pulse shape behavior. Isolated pulses were used so that this loss response does not reflect the effects of nonlinear intersymbol interference (e.g., partial erasure [11]). The envelope, as defined by the amplitude of the fundamental and the odd harmonics of the measured spectrum is linear for frequencies up to 5 MHz, after which the measured response decreases significantly. The frequency of this breakpoint coincides with the frequency in Fig. 8 where the ac-erasure-induced noise response deviates from the calculated response. Hence, the discrepancy observed in Fig. 8 is not due to any fundamental flaw in the Poisson model, and using a more accurate head representation to account for

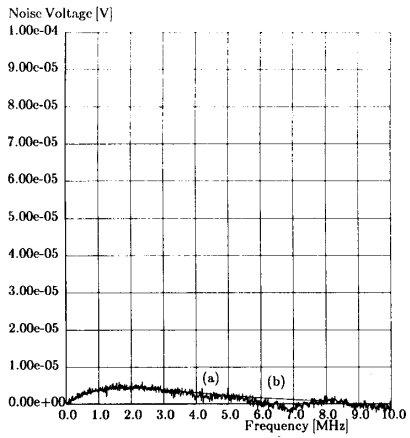

Fig. 10. Experimental data for disk *C*: (*a*) measured bulk-erasure-induced noise data; and (*b*) peak-amplitude-normalized channel response.

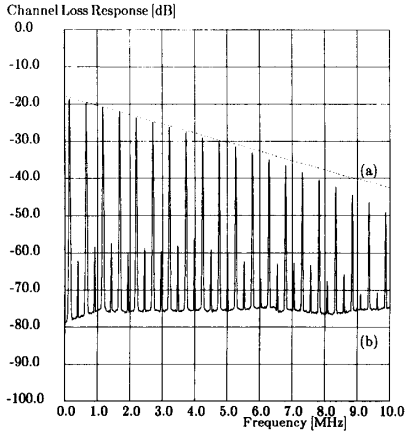

Fig. 11. (*a*) Envelope for power spectrum of a sequence of Lorentzian pulses, and (*b*) measured channel loss response.

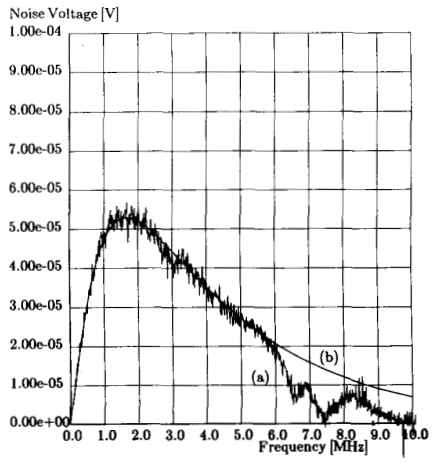

Fig. 12. (*a*) Measured head-erasure-induced noise data, and (*b*) model curve fit to data.

the added bandwidth losses should extend the capability of the model described by (11).

Curves were fitted to the data shown in Figs. 8 and 9 with respect to the parameter σ, using the moderately high frequency region. It is noted that σ, which is approximately $d + a$ where d is the head–medium spacing and a is the recording-transition parameter, for an ac-erasure-induced transition equals the recording-head-induced transition parameter when the width of the transition is governed by self-demagnetization. The data indicate that values for σ_{fitted} for ac-erasure-induced noise agree with σ_{jitter}, as shown in Fig. 6, so that the jitter-noise recording-transition width equals the ac-erasure-induced noise recording-transition width. Further, σ_{fitted} is approximately equal to σ_{PW50} so that the transition widths of the recorded and induced transitions appear to be limited by self-demagnetization and not limited, for example, by head-field gradients.

Curves were fitted to the data with the model with respect to frequency of the peak response, to obtain values for λ, $E\{M\}$, and $V\{M\}$. It is noted that the coefficient α was defined by the channel at low frequencies, and that σ was defined as above, so that λ, $E\{M\}$, and $V\{M\}$ become parameters of the model. The curve fitting was performed by first conducting a correlation of the form

$$\rho^2 = \frac{\left(\sum_{i=1}^{N} D(\omega_i)\, S(\omega_i)\right)^2}{\sum_{i=1}^{N} D^2(\omega_i) \sum_{i=1}^{N} S^2(\omega_i)} \qquad (13)$$

where $S(\omega_i)$ is the function given by (12) and $D(\omega_i)$ is the function containing the noise data as shown in Figs. 8 and 9. The sums were computed at discrete frequencies ω_i, since the data were digitized as a discrete function of frequency, over the frequency band where the data and (12) were in agreement, i.e., from dc to 5.0 MHz.

The correlations were performed by first setting $V\{M\} = 0$, and determining ρ as a function of λ. The peak values of $\rho(\lambda)$ provide the best estimate of λ, λ_{est}, as shown in Table IV. Correlations in excess of 0.9987 were obtained, suggesting that the contribution of the variance is minimal. The ratio of the two sums in the denominator of (13) then provided an estimate for $E\{M\}$. Using these values of λ and $E\{M\}$, the function $S(\omega_i)$ was computed and subtracted from $D(\omega_i)$, producing a function η, which should contain the variance-dependent component. A correlation was then performed on η using (12) and (13) for $E\{M\} = 0$. However, a peak in $\rho(\lambda)$ was not observed at $0.5\lambda_{\text{est}}$, as would be expected. The noisiness of the data may have limited the ability to estimate the minute variance. Future work would involve devising and completing a suitably sensitive experiment to allow the variance, if any, to be estimated. For the present, the value of the variance is taken to be zero. Under this condition, the random process $m(t)$ appears as a binary process.

The value of λ for these thin-film disks is in the range of 2 to 4 MHz, indicating that this is the expected value for the frequency of the ac-erasure-induced transitions. Further, the model uses the value of λ to define the frequency of transitions between magnetized regions of differing coercivity. Hence, it is inferred that the variation in coercivity within each magnetized region is negligible, and that the parameter λ can be used as a measure of the uniformity of the medium.

The curves fitted for $E\{M\}$ (where the $V\{M\}$ term is neglected) agreed well with the data, showing that although Poisson statistics are needed to describe the noise statistics along the track direction, it is sufficient to invoke the concept of an average magnetization to describe the measured noise statistics along the track width. The value of $E\{M\}$ due to the averaged transitions induced by the ac-erasure process was smaller than the signal amplitudes which are due to saturated transitions by a factor approaching one thousand. The small value of $E\{M\}$ implies that only relatively small amounts of net flux, compared to the flux which can be made to reach the head, are reaching the head. This small value of $E\{M\}$ could be due to the overall cancellation of oppositely directed components of the longitudinally directed flux, or could be attributed in part to the occurrence of flux closure in the medium. Hence, while the model is seen to represent accurately the readback flux, the model may or may *not* be representing the actual state of the magnetization throughout the disk. This does not suggest that the model in itself is incorrect, but is rather a statement about the nature of Reciprocity and Riemann Integrals. By Reciprocity, given a magnetization distribution and a head field representation, a single flux and, hence, signal distribution may be created; but a given flux distribution and a head field representation do not, in turn, uniquely determine the magnetization.

The small value of variance $V\{M\}$ is attributed to the effect of the Central Limit Theorem, in that the width of a recording head senses a large number of magnetized regions at any instant in time. Since the variance sensed by the recording head is the variance of individual magnetized regions divided by the number of magnetized regions, it is reasonable that the measured variance would be quite small.

It can be seen from (11) that under the limiting condi-

tions of either very large σ or very large λ, $S_m(\omega)$ is constant with respect to $H(\omega)$. Hence, under these limiting conditions, the noise from erasure-induced transitions behaves like white noise at the input of the recording channel.

The ac-erasure-induced noise for a particulate disk *C* is shown in Fig. 10(*a*). A curve fit simply to the response of the channel is shown in Fig. 10(*b*). The similarity of the fit to the data indicates that the ac-erasure-induced noise indeed appears as a white-noise process [1], [2] or as a Poisson process with a large Poisson parameter whose lower bound can only be estimated. This estimate for λ is based on assuming that the value of λ is sufficiently large so that $4\lambda^2 + \omega^2$, in (7), between dc and some maximum frequency, e.g., 5.0 MHz, changes by less than some amount, e.g., 10 percent. Such an estimate suggests that λ for particulate disks is at least a factor of ten greater than λ for thin-film disks as indicated in Table IV, and corresponds to dimensions on the order of or less than the particle size.

The ac-erasure-induced noise for thin-film disk *A* was measured additionally for when the erasure was induced with a recording head, as shown in Fig. 12(*a*). The curve fitted in Fig. 12(*b*) is in agreement with the data, and suggests that the model may be applied to the readback noise properties of both recording-head-induced and bulk-induced ac erasure.

The curve fitted in Fig. 12(*b*) to the data in Fig. 12(*a*) differs from the curve fitted to the data in Fig. 8 in that although the value of $E\{M\}$ was somewhat reduced, λ had to be increased by more than a factor of two. This significant increase could be due to the greater number of induced transitions due to the larger field gradient of the head. Another interpretation is based on the treatment of signal-dependent modulation noise as a white-noise process [11], as depicted in Fig. 6. If the high-frequency erasure due to the recording head is treated as signal writing, then the value of λ should increase to the extent that demagnetizing effects in the disk limit the increase. The finite value for λ in these data then indicates that demagnetization effects, as seen in Fig. 8, are significant.

It is also noted that the effects of excess noise properties [18] are not apparent in Fig. 12. This type of noise may be associated with track edges in thin-film media and therefore alter the noise statistics along the width of the track. Due to the similarity of the bulk-erasure and head-erasure spectra, the assumption of uniform noise statistics across the width of the track is supported at the level of sensitivity of these experiments for these wide-track recording heads.

In deriving the present model, it was assumed that $m(t)$ changed sign whenever any transition was encountered. In general, $m(t)$ must only change in value, and not necessarily in sign, to form a source of diverging magnetization. A new analysis would need to be considered to account for this case. However, the agreement between the present model and data suggests that this effect may be observable only at significantly higher frequencies or at higher sensitivities, and that the present model accounts for much of the observed noise spectra.

VII. Conclusions

It has been shown that noise in thin-film media may be induced with decaying ac magnetic fields. A comparison between the model and experiments indicates that this ac-erasure-induced noise in thin-film media has positional statistics along the track length which follow a Poisson process model; where the noise statistics along the track width may be assumed to be uniform, with an average value that has small variance. This noise in particulate media follows white-noise statistics, or, equivalently, follows a Poisson process with a large Poisson parameter. Values for the Poisson parameter and the effective transition amplitude have been measured experimentally for a set of thin-film and particulate disks.

Appendix
Derivation of Equation (6)

Let the number of transitions in the time interval $(t, t+\tau)$ be k. Also, let τ be positive, so that the length of the interval is τ. Then, the autocorrelation function is expanded into the following terms:

$$
\begin{aligned}
R_m(\tau) &= E\{m(t)\, m(t+\tau)\} \\
&= E\{m(t)\, m(t+\tau) \mid m(t) > 0,\, m(t+\tau) > 0,\, k = 0\} \cdot P\{m(t) > 0\} \cdot P\{k = 0\} \\
&\quad + E\{m(t)\, m(t+\tau) \mid m(t) < 0,\, m(t+\tau) < 0,\, k = 0\} \cdot P\{m(t) < 0\} \cdot P\{k = 0\} \\
&\quad + E\{m(t)\, m(t+\tau) \mid m(t) > 0,\, m(t+\tau) > 0,\, k \neq 0,\, k \text{ even}\} \cdot P\{m(t) > 0\} \cdot P\{k \neq 0,\, k \text{ even}\} \\
&\quad + E\{m(t)\, m(t+\tau) \mid m(t) < 0,\, m(t+\tau) < 0,\, k \neq 0,\, k \text{ even}\} \cdot P\{m(t) < 0\} \cdot P\{k \neq 0,\, k \text{ even}\} \\
&\quad + E\{m(t)\, m(t+\tau) \mid m(t) > 0,\, m(t+\tau) < 0,\, k \text{ odd}\} \cdot P\{m(t) > 0\} \cdot P\{k \text{ odd}\} \\
&\quad + E\{m(t)\, m(t+\tau) \mid m(t) < 0,\, m(t+\tau) > 0,\, k \text{ odd}\} \cdot P\{m(t) < 0\} \cdot P\{k \text{ odd}\} \\
&= E\{M^2\}\, e^{-\lambda t} \cosh \lambda t e^{-\lambda\tau} + E\{M^2\}\, e^{-\lambda t} \sinh \lambda t e^{-\lambda\tau} + E\{M\}^2 e^{-\lambda\tau} [\cosh \lambda\tau - 1] e^{-\lambda t} \cosh \lambda t \\
&\quad + E\{M\}^2 e^{-\lambda\tau} [\cosh \lambda\tau - 1] e^{-\lambda t} \sinh \lambda t - E\{M\}^2 e^{-\lambda\tau} \sinh \lambda\tau e^{-\lambda t} \cosh \lambda t \\
&\quad - E\{M\}^2 e^{-\lambda\tau} \sinh \lambda\tau e^{-\lambda t} \sinh \lambda t \\
&= [E\{M^2\} - E\{M\}^2]\, e^{-\lambda\tau} + E\{M\}^2 e^{-2\lambda\tau} \\
&= V\{M\}\, e^{-\lambda\tau} + E\{M\}^2 e^{-2\lambda\tau}. \qquad (14)
\end{aligned}
$$

The above expression for the autocorrelation function is valid only for positive values of τ. If τ is negative, the length of the time interval $(t, t + \tau)$ equals $-\tau$. Hence, for $\tau < 0$

$$R_m(\tau) = V\{M\}\, e^{\lambda\tau} + E\{M\}^2 e^{2\lambda\tau}. \qquad (15)$$

Equation (6) follows from (14) and (15).

Acknowledgment

The authors would like to thank the Applied Magnetics, Komag, Lin Data, and Nashua Corporations for supplying the heads and media used in this study, and J. J. Moon for helpful discussions.

References

[1] J. C. Mallinson, "Maximum signal-to-noise ratio of a tape recorder," *IEEE Trans. Magn.*, vol. MAG-5, no. 3, pp. 182–186, Sept. 1969.
[2] G. F. Hughes and R. K. Schmidt, "On noise in digital recording," *IEEE Trans. Magn.*, vol. MAG-12, no. 6, pp. 752–754, Nov. 1976.
[3] V. V. Veeravalli, R. R. Katti, B. V. K. Vijaya Kumar, and M. H. Kryder, "Time-domain model for noise from particulate recording media," *J. Appl. Phys.*, vol. 61, no. 8-IIB, pp. 4034–4036, 1987.
[4] Y. S. Yang, "Noise autocorrelation in magnetic recording systems," *IEEE Trans. Magn.*, vol. MAG-21, no. 5, pp. 1389–1391, Sept. 1985.
[5] A. Anzaloni and L. Barbosa, "The average power density spectrum of the readback voltage from particulate media," *IEEE Trans. Magn.*, vol. MAG-20, no. 5, pp. 693–696, Sept. 1984.
[6] L. Thurlings, "Statistical analysis of signal and noise in magnetic recording," *IEEE Trans. Magn.*, vol. MAG-16, no. 3, pp. 507–513, May 1980.
[7] R. A. Baugh, E. S. Murdock, and B. R. Natarajan, "Measurement of noise in magnetic media," *IEEE Trans. Magn.*, vol. MAG-19, no. 5, pp. 1722–1724, Sept. 1983.
[8] N. R. Belk, P. K. George, and G. S. Mowry, "Noise in high performance thin-film longitudinal magnetic recording media," *IEEE Trans. Magn.*, vol. MAG-21, no. 5, pp. 1305–1355, Sept. 1985.
[9] T. C. Arnoldussen, "Thin-film recording media," *Proc. IEEE*, vol. 74, no. 11, pp. 1526–1539, Nov. 1986.
[10] M. Madrid and R. Wood, "Transition noise in thin-film media," *IEEE Trans. Magn.*, vol. MAG-22, no. 5, pp. 892–894, Sept. 1986.
[11] J. J. Moon, L. R. Carley, and R. R. Katti, "Density dependence of noise in thin metallic longitudinal media," in *Proc. 1987 MMM Conf.* (Chicago, IL), Apr. 1988.
[12] H. Aoi, M. Saitoh, N. Nishiyama, R. Tsuchiya, and T. Tamura, "Noise characteristics in longitudinal thin-film media," *IEEE Trans. Magn.*, vol. MAG-22, no. 5, pp. 895–897, Sept. 1986.
[13] H. N. Bertram, K. Hallamasek, and M. Madrid, "DC-modulation noise in thin metallic media and its application for head efficiency measurements," *IEEE Trans. Magn.*, vol. MAG-22, no. 4, pp. 247–252, July 1986.
[14] A. Papoulis, *Probability, Random Variables, and Stochastic Processes*, 2nd ed. New York, NY: McGraw-Hill, 1984.
[15] R. I. Potter, "Analysis of saturation magnetic recording based on arctangent magnetization transitions," *J. Appl. Phys.*, vol. 41, no. 4, pp. 1647–1651, Mar. 1970.
[16] H. N. Bertram, "Fundamentals of the magnetic recording process," *Proc. IEEE*, vol. 74, no. 11, pp. 1494–1512, Nov. 1986.
[17] O. Karlqvist, "Calculation of the magnetic field in the ferromagnetic layer of a magnetic drum," *Trans. Roy. Inst. Technol. Stockholm*, no. 86, 1954.
[18] E. J. Yarmchuk, "Spatial structure of media noise in film disks," *IEEE Trans. Magn.*, vol. MAG-22, no. 5, pp. 877–882, Sept. 1986.

Romney R. Katti (S'83–M'87) was born in Tallahassee, FL, on September 9, 1961. He received the B.S. degree with Honors in engineering and applied science from the California Institute of Technology, Pasadena, in 1982, and the M.S. degree in electrical engineering from Stanford University, Stanford, CA, in 1983, and the Ph.D. degree in electrical engineering at Carnegie Mellon University, Pittsburgh, PA, in 1988.

He was a research assistant at the Magnetics Technology Center at Carnegie Mellon. He is now at the Jet Propulsion Laboratory, Pasadena, CA.

Dr. Katti is a member of Tau Beta Pi, the IEEE Magnetics Society, and Sigma Xi.

Venugopal V. Veeravalli was born in India on July 28, 1963. He received the B.Tech (first class with distinction) degree from the Indian Institute of Technology, Bombay, India, in 1985, and the M.S. degree from Carnegie Mellon University, Pittsburgh, PA, in 1987, both in electrical engineering.

He is currently working towards the Ph.D. degree in electrical engineering at the University of Illinois at Urbana-Champaign, where he is also a Research Assistant at the Coordinated Science Laboratory.

Mark H. Kryder (M'79–SM'87) was born in Portland, OR, on October 7, 1943. He received the B.S. degree in electrical engineering from Stanford University, Stanford, CA, in 1965 and the M.S. and Ph.D. degrees in electrical engineering and physics from the California Institute of Technology, Pasadena, in 1966 and 1970, respectively.

From 1969 to 1971 he was a Research Fellow at the California Institute of Technology. From 1971 to 1973 he was a Visiting Scientist at the University of Regensburg, West Germany; and from 1973 to 1978 he was a member of the Research Staff and Manager of Exploratory Bubble Devices at the IBM T. J. Watson Research Center, Yorktown Heights, NY. In 1978 he joined the faculty at Carnegie Mellon University, Pittsburgh, PA where he is Professor of Electrical and Computer Engineering and Director of the Magnetics Technology Center, which he founded. He has over one hundred publications and eight patents in the area of magnetic memory technology. His current research interests include magnetic recording, magnetooptical recording, and magnetic bubble technology.

Dr. Kryder has been a member of the IEEE Magnetics Society and the American Physical Society for over twenty years, is currently a member of the IEEE Magnetics Society Conference Executive Committee, was a Distinguished Lecturer for the Society in 1985 and has served on the management committees of a number of Intermag and Magnetism and Magnetic Materials Conferences. He was publications co-chairman at the 1981 Intermag in Grenoble, program co-chairperson of the 1982 Joint MMM-Intermag Conference in Montreal, and General Chairman of the 1987 Intermag Conference in Tokyo.

B. V. K. Vijaya Kumar (S'78–M'80) received his Bachelor of Technology and Master of Technology degrees in electrical engineering from the Indian Institute of Technology, Kanpur, in 1975 and 1977, respectively.

After completing the Ph.D. requirements in electrical engineering at Carnegie Mellon University (CMU), Pittsburgh, PA, in 1980, he worked for two years as a research associate at CMU. He joined the Department of Electrical and Computer Engineering at CMU in 1982 as an Assistant Professor and is currently an Associate Professor. His research interests are primarily in optical data processing, pattern recognition, and magnetic recording. He has published more than 80 technical papers. He is listed in Marquis's *Who's Who in Optical Sciences and Engineering*.

Dr. Vijaya Kumar is a member of OSA, SPIE, Sigma Xi, and INNS (International Neural Networks Society). He was also chairman of the 1988 Max Born Award Committee for the Optical Society of America.